Artificial Intelligence In Medicine xxx (xxxx) xxx–xxx

Contents lists available at ScienceDirect

Artificial Intelligence In Medicine

journal homepage: www.elsevier.com/locate/artmed

CT liver tumor segmentation hybrid approach using neutrosophic sets, fast fuzzy c-means and adaptive watershed algorithm

Ahmed M. Anter[a,c,*], Aboul Ella Hassenian[b,c]

[a] Faculty of Computers and Information, Beni-Suef University, Benisuef, Egypt
[b] Faculty of Computers and Information, Cairo University, Cairo, Egypt
[c] Scientific Research Group in Egypt (SRGE), Egypt[1]

A B S T R A C T

Liver tumor segmentation from computed tomography (CT) images is a critical and challenging task. Due to the fuzziness in the liver pixel range, the neighboring organs of the liver with the same intensity, high noise and large variance of tumors. The segmentation process is necessary for the detection, identification, and measurement of objects in CT images. We perform an extensive review of the CT liver segmentation literature. Furthermore, in this paper, an improved segmentation approach based on watershed algorithm, neutrosophic sets (NS), and fast fuzzy c-mean clustering algorithm (FFCM) for CT liver tumor segmentation is proposed. To increase the contrast of the liver CT images, the intensity values are adjusted and high frequencies are removed using histogram equalization and median filter approach. It is followed by transforming the CT image to *NS* domain, which is described using three subsets (percentage of truth *T*, the percentage of indeterminacy *I*, and percentage of falsity *F*). The obtained *NS* image is enhanced by adaptive threshold and morphological operators to focus on liver parenchyma. The enhanced *NS* image passed to a watershed algorithm for post-segmentation process and liver parenchyma is extracted using the connected component algorithm. Finally, the liver tumors are segmented from the segmented liver using fast fuzzy c-mean (FFCM). A quantitative analysis is carried out to evaluate segmentation results using six different indices. The results show that the overall accuracy offered by the employed neutrosophic sets is accurate, less time consuming, less sensitive to noise and performs better on non-uniform CT images.

1. Introduction

Liver tumors are the most common internal malignancies worldwide and also one of the leading death causes. Early detection, diagnosis and accurate staging of liver cancer is an important issue in radiography. In a CT scan, manual segmentation is tedious and prohibitively time-consuming for a clinical setting. Automatic liver tumor segmentation is a very challenging task, due to various factors: liver stretch over 150 slices in a CT DICOM file, indefinite shape of the lesions, low-intensity contrast between lesions and similar to those of nearby tissues, irregularity in the liver shape and size between patients and the similarity with other organs make automatic liver segmentation very difficult [1].

Several types of research have developed various algorithms for image segmentation that can be categorized based on the degree of automation (semi, interactive or fully). The most popular segmentation approaches are histogram-based methods, region-based methods, edge-based methods, model-based methods, watershed methods, fuzzy logic methods. As shown in Table 1, each of these approaches has its advantages and disadvantages in terms of applicability, suitability, performance, and computational cost [2,3].

In some applications such as expert systems, we should consider not only the truth membership but also the falsity of membership and the indeterminacy of the two memberships. It is hard for the fuzzy set to solve such problems [4]. Neutrosophic logic (NL) is a generalization of fuzzy logic (FL) and carries more information than FL. NL introduces a new indeterminacy set due to unexpected hidden parameters in some propositions [5].

Particularly, no one who did not consider the above characteristics of the abdominal CT image can meet desirable results in liver and tumor segmentation. Therefore, to address the above-mentioned problems, we proposed a fully automatic liver tumor segmentation approach from abdominal CT scans based on watershed, neutrosophic sets, and fast fuzzy c-mean.

The proposed approach is comprised of five phases. In the first phase, CT image is converted to gray-scale, contrast-enhanced using histogram equalization and noise removed by applying a median filter approach. In the second phase, the image is transformed to NS domain. Each pixel in *NS* belongs to either Truth or False or Indeterminate subsets. The image becomes more uniform, homogeneous, and more suitable for the segmentation process. In the third phase, morphological operators open and reconstruct are used to delete small objects and focus on liver parenchyma. In the fourth phase, the algorithm marks foreground and background objects from truth image based on neutrosophic set and watershed algorithm to segment CT images. Then the

* Corresponding author.
[1] http://www.egyptscience.net.

https://doi.org/10.1016/j.artmed.2018.11.007
Received 14 March 2018; Received in revised form 9 September 2018; Accepted 25 November 2018
0933-3657/

Table 1
Summary of segmentation methods.

Methods	Advantages	Disadvantages
Histogram-based	Fast and simple	Difficult to identify significant peaks and valleys
Edge-based	Fast and well developed	Edges are often disconnected
Region-based	The concept is simple. Multiple stop criteria can be chosen	The choice of seeds is important and critical. Sensitive to noise
Model-based	Finds certain-shaped regions	The regions need to fit a certain model
Watershed	The boundaries of each region are continuous. No seed is needed. Resulting regions are connected	Sensitive to noise and non-homogeneity. The algorithm is time-consuming and over-segmentation problem
Clustering-based	Fuzzy set is a rule-based segmentation and takes into account the uncertainty and fuzziness	Affected by the number of initial clusters
Machine learning	Stable, different lesion characteristics can be incorporated by feature extraction	Long training time; over-training problem; test images should come from the same platform as the training images

connected component algorithm is used to select and extract liver from abdominal CT. Finally, the segmented liver passed to fast fuzzy c-mean clustering algorithm to segment and detect tumors.

The remainder of this paper is ordered as follows. Section 2 explains the related work. Section 3 explains the methodology of the proposed approach. In Section 4, the segmentation approach based on the new Neutrosophic set, Watershed algorithm and Fast-fuzzy c-means is proposed. The experimental results and analysis with details of the datasets are discussed in Section 5. Finally, conclusion and future work are discussed in Section 6.

2. State of the art

Nowadays several works have been proposed at the state of the art, which effectively solve the problems of liver tumor segmentation from abdominal CT scans. They can be broadly grouped into two approaches, (1) direct approaches that segments tumor alone and (2) indirect approaches that *segment* liver first and then segment tumor from it.

Direct approaches, Moltz et al. in [6] proposed a hybrid method for tumor segmentation. It performs a coarse segmentation by adaptive thresholding based on a gray value and removes structures adjacent to the tumor by model-based morphological processing. The method requires the user to specify the center of the region of interest (ROI). Wong et al. in [7] proposed a semi-automatic method based on region growing with knowledge-based constraints to segment tumors from CT slices. Knowledge-based constraints are introduced to ensure that the size and the shape of the region grown lies within acceptable parameters. The method requires an ROI was determined manually by selecting two points on the CT image prior to region growing. Li et al. [8] proposed an integrated method with FCM and level set method for liver tumor segmentation. The initial segmentations obtained by FCM and the fine delineation obtained with level set method were interfaced by morphological operations. The limitation of this method is that the level set method requires high processing time. Smeets et al. in [9] used the level set function for tumor segmentation. The algorithm is initialized by a spiral scanning technique based on the seed point placed inside the tumor. The level set evolves according to a speed image obtained by statistical pixel classification with supervised training. The algorithm requires the user to select a point at the center of the tumor and to specify a maximal radius by placing a point in the surrounding liver tissue. Moghe et al. in [10] proposed an automatic threshold-based liver tumor segmentation method from CT images. The method uses a lower threshold and a higher threshold; that was determined from statistical moments and texture measures, however, the selection of threshold values is difficult in this method.

All methods in the direct approach need for user intervention to support the segmentation process. This intervention is not desirable for the automatic segmentation of tumor. As regards indirect approaches, the tumor segmentation starts with segmenting the liver first from CT images. Segmentation of tumor from the segmented liver simplifies the segmentation problem by decreasing the computational time and decreasing the number of possible external organs during the segmentation process.

For liver segmentation, Nural and Hans in [11] proposed approach depend on integration of morphology and graph-based techniques for liver segmentation. It uses anisotropic diffusion, adaptive threshold based on prior knowledge and connected component algorithm to segment tumors from the segmented liver. While, Kumar et al. in [12], proposed an approach for automatic and effective segmentation of liver lesion from CT images. The method uses confidence connected region growing for automatic segmentation of liver and alternative fuzzy c-means clustering for lesion segmentation. The algorithm applied on 10 cases of abdominal CT scans.

Badura and Pietka in [13], proposed a semi-automated method for segmentation of liver in CT, the proposed system consists of the three-dimensional anisotropic diffusion filtering and the adaptive region growing, supported by the fuzzy inference system. The system has been evaluated using 17 abdominal CT scans yielding 77% effectiveness.

Lim et al. in [14], proposed an unsupervised liver segmentation algorithm with three steps. In the pre-processing, the CT image is simplified by estimating the liver position using a prior knowledge and performing multi-level threshold on the estimated liver position. The proposed scheme utilizes the multi-scale morphological filter recursively with region-labeling and clustering to detect the search range for deformable contouring. In order to perform an accurate segmentation, the gradient label map is produced. Experimental results are compared with manually segmented images by a radiologist and shown to be efficient. Huang et al. in [15] proposed hybrid approach for automatic liver segmentation. At first liver intensity range is detected based on prior knowledge of liver volume. Then ROI is extracted using atlas-based affine and non-rigid registration. At the last step, to achieve more accurate segmentation, major liver tumors are detected using a gray level and distance prior knowledge, and then a modified diffeomorphic demons registration with shape constraint is applied. Results show that the proposed approach can be a potential tool in clinical application.

Jeongjin et al. in [16] proposed two steps seeded region growing (SRG) onto level-set speed images to define an approximate initial liver boundary. The first SRG efficiently divides the CT image into a set of discrete objects based on the gradient information and connectivity. The second SRG detects the objects belonging to the liver based on dimensional shape propagation. Experimental results show that the proposed system fast, converge to the optimal position and accurate for liver volume segmentation. Ruchaneewan et al. in [17] proposed approach consists of four stages: in the first stage, an intensity-based is applied to obtain soft tissue. In the second stage, a region-based texture classification is used to classify all the soft tissue regions. During the third stage, an initial region of the liver for each patient is determined from the probability images. In the final fourth stage, a 95% confidence interval determined from the intensities of the initial regions is used to detect the liver region.

Campadelli et al. in [18] proposed fully automatic liver segmentation and reviewed different liver segmentation techniques in [19]. They

described their method as a low computational cost gray-level based technique where no data samples are needed. Furthermore, all employed parameters are not crucial. Some parameters are based on anatomical information, while the rest of the parameters have been guided by reasoning. The method implementation starts with the heart volume segmentation based on a priory anatomical knowledge. Then, five labeled partitions of the abdominal volume are selected. These partitions are used to calculate a set of parameters to create the edge map to detect the image details. All the information and parameters are employed with the region growing algorithm to segment the abdomen organs based on the assumption that the gray levels for each organ follow a Gaussian distribution.

Lu et al. in [20], proposed automated liver segmentation based on support vector machine (SVM) and texture description. 28 liver CT dataset is used in experiments. Images Segmentation process started with texture classification. The wavelet transform is used to drive input to support vector machine which classified pixels in the liver and non-liver region. The segmented liver is still not smoothed and still need some improvement. For the refinement of results authors used region growing method. For refining holes and broken areas within the liver, dilation is used. Misclassified pixels outside the liver are removed by erosion.

Kaur et al. in [21], proposed enhanced K-means clustering algorithm for liver image segmentation. 20 liver CT dataset are used with resolution 512 × 512. K-means divides given CT image to a number of clusters. In K-means process, K-centroids are defined one for each cluster. The main drawback is that attached organs are not removed properly. So morphological opening-by-reconstruction is used to improve the performance. The proposed method compared with region growing and showed that enhanced K-means provides better results than region growing.

Zhao et al. in [22], proposed new liver image segmentation algorithm combining fuzzy C-means and multi-layer perceptron. The dataset contains 40 slices for 10 patients are used with resolution 320 × 320. Threshold method is used for enhancing the quality of image. Fuzzy c-mean clustering and morphological reconstruction filter are used to delineate initial liver boundary. This segmented image is used to train a multilayer perceptron neural network. The process is repeated until all the slices images have been segmented.

For liver tumor segmentation. Hame in [23] proposed a method to segment tumors in two stages. The liver is segmented using simple thresholding and morphological operations, from which a rough segmentation of tumors is obtained. The rough segmentation result is refined using a fuzzy clustering approach and the final tumor segmentation is obtained by fitting a geometric deformable model, based on the membership function generated by the clustering. Ciecholewski and Ogiela in [24] proposed contour modeling to segment the liver from CT images. The resulting image was enhanced by histogram transformation to find lesions.

Taieb et al. in [25] proposed a method to segment liver and tumors from abdominal CT images. The method repeatedly applies multi-resolution, multi-class smoothed Bayesian classification followed by morphological adjustment and active contours refinement for segmentation. Intensity distribution function for liver and tumor are computed using multiclass and pixel neighborhood information. Initially, rectangular region around a manually selected seed inside the liver and additional seeds inside the liver tumors are computed and interpreted as the parameters of the liver and tumor classes.

Zhang et al. in [26] proposed an interactive method for liver tumor segmentation from CT images. The liver was segmented first using preprocessing operations and then watershed transform was employed to partition the CT volume into the large number of catchment basins. Then, the tumors were extracted from the segmented liver by training a support vector machine (SVM) classifier based on the user selected seed points. The corresponding features for training and prediction were computed using the small regions extracted by the watershed transform. This method requires manual selection of seed points. Patil et al. in [27] proposed approach to segment tumors in the two-level operations. First level Segmentation of liver is performed by using two methods of adaptive threshold with morphological operations and global threshold with morphological operations. Second level tumor Segmentation, three methods were used in that level adaptive threshold with morphological operations, Fuzzy C Mean Clustering and Region Growing. The proposed approach compares and selects the best of all and produces the final result. It is improving the accuracy of the segmentation for distinct quality and category of CT images. Kumar and Moni in [28] used adaptive threshold and morphological processing for liver segmentation. Each suspicious tumor region was automatically extracted from the segmented liver using the fuzzy c-mean technique. Also, neural network is used to identify normal liver and abnormal liver region in [29], 10 liver CT scans with resolution 512 × 512 are used, a histogram equalization is used to increase the quality and contrast of images. In the feature extraction step, five set of features are extracted using statistically based features, intensity based approach, morphological based features, frequency domain based and wavelet domain based features. Principal component analysis (PCA) is used for feature selection. A feed-forward multi-layer perceptron is trained using back propagation algorithm for the selected features to take the decision.

Most of these methods are time-consuming and do not respond identically to different patients. They usually produce over segmentation and also give unsatisfied results for the slices with fuzzy liver boundary. The tumor segmentation is inaccurate for different volume and shapes. In this paper, an automatic and effective algorithm that segments liver and tumors from CT scans is proposed using a hybrid segmentation approach based on neutrosophic sets, watershed algorithm, and fast fuzzy c-means.

3. Preliminaries

This section provides a brief explanation of liver CT imaging technology, Pre-processing, morphological operator, watershed algorithm, and neutrosophic sets along with some of the key basic concepts. A more comprehensive review can be found in sources such as [30–33].

3.1. Neutrosophic sets (NS)

Neutrosophy is a branch of philosophy, introduced by Florentin in 1995, which includes four fields: philosophy, logic, set theory, and probability. Neutrosophic set and its properties are discussed briefly in [5]. The problems which cannot be solved by FL, the NL can solve it. NS studies the neutrosophic logical values of the propositions that represented by subsets (truth (T), indeterminacy (I), and falsity (F)) [32].

Definition 1 (*Neutrosophic set*). define T, I, and F as neutrosophic components. Let T, I, and F be standard or non-standard real subsets of $]^{-}0,1^{+}[$. An element $A(T, I, F)$ belongs to the set in the following way: it is t true ($t \in T$), i indeterminate ($i \in I$), and f false ($f \in F$), where t, i, and f are real numbers [33].

In order to apply neutrosophy, an image needs to be transferred to a neutrosophic domain P_{NS}. A pixel in the neutrosophic domain can be represented as T, I, and F meaning the pixel is t% true, i% indeterminate, and f% false, where t varies in T, i varies in I, and f varies in F, respectively. In a neutrosophic set, $0 \le t, i, f \le 1$. However, in a classical set, $i = 0$, t and f are either 0 or 1 and in a fuzzy set, $i = 0$, $0 \le t, f \le 1$ [30]. The pixel $P(i, j)$ in the image domain is transformed into neutrosophic domain $P_{NS}(i, j)$ which is represented by $T(i, j)$, $I(i, j)$, $F(i, j)$ and calculated as follow:

$$P_{\mathrm{NS}}(i,j) = \{T(i,j), I(i,j), F(i,j)\} \tag{1}$$

$$T(i,j) = \frac{g(\bar{i},j) - \bar{g}_{\min}}{\bar{g}_{\max} - \bar{g}_{\min}} \tag{2}$$

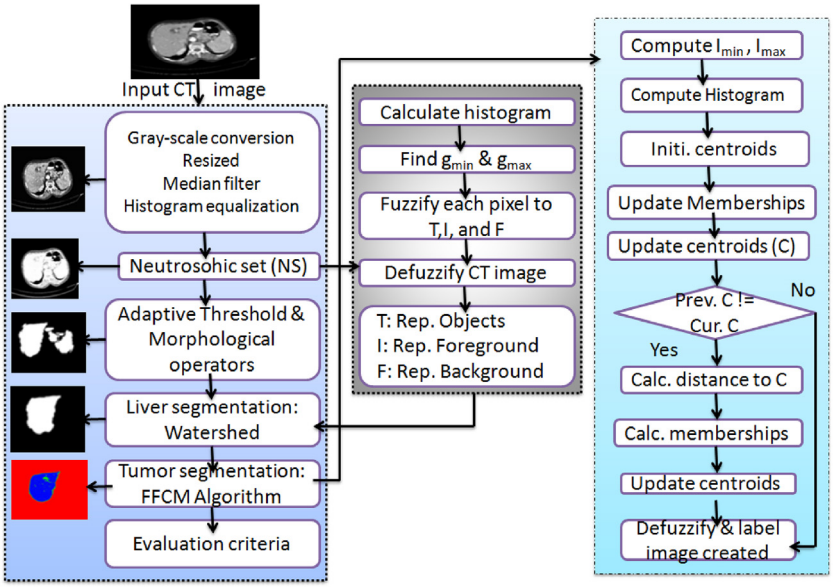

Fig. 1. Proposed approach phases for automatic liver tumor segmentation.

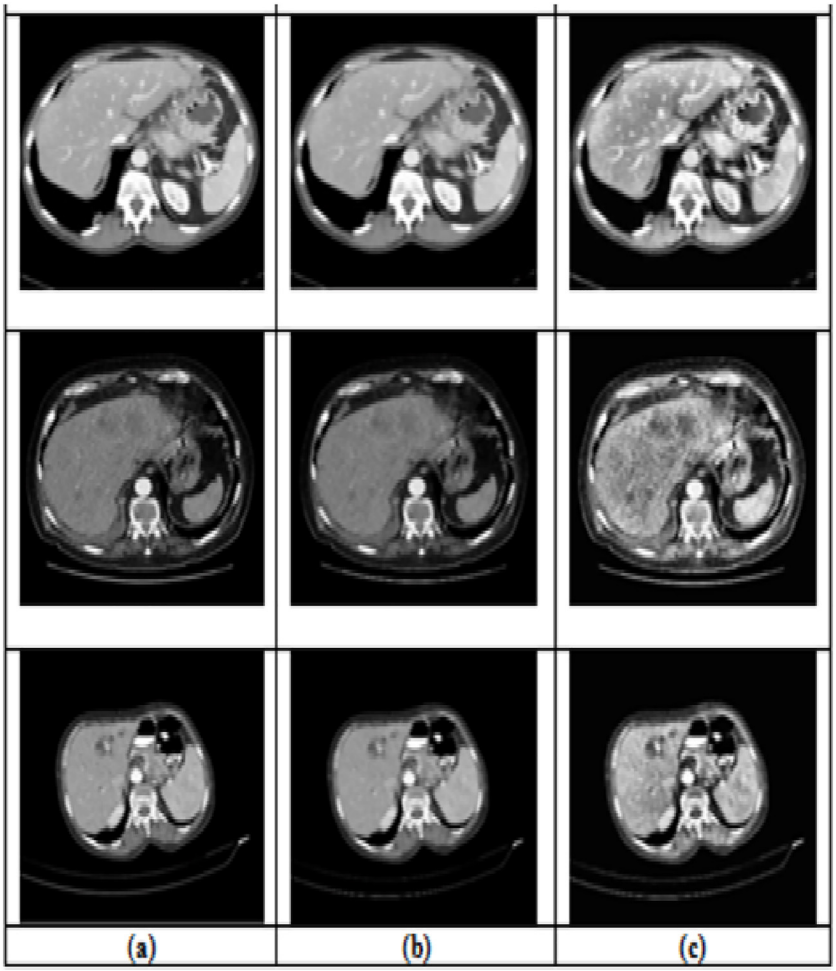

Fig. 2. Results of different cases abdominal CT images after enhancement. (a) Original image, (b) image after applying median filter, and (c) image after apply histogram equalization.

$$I(i,j) = 1 - \frac{\mathrm{Ho}(i,j) - \bar{\mathrm{Ho}}_{\min}}{\bar{\mathrm{Ho}}_{\max} - \bar{\mathrm{Ho}}_{\min}} \tag{3}$$

$$F(i,j) = 1 - T(i,j) \tag{4}$$

$$\mathrm{Ho}(i,j) = \mathrm{abs}(g(i,j) - g(\bar{i},j)) \tag{5}$$

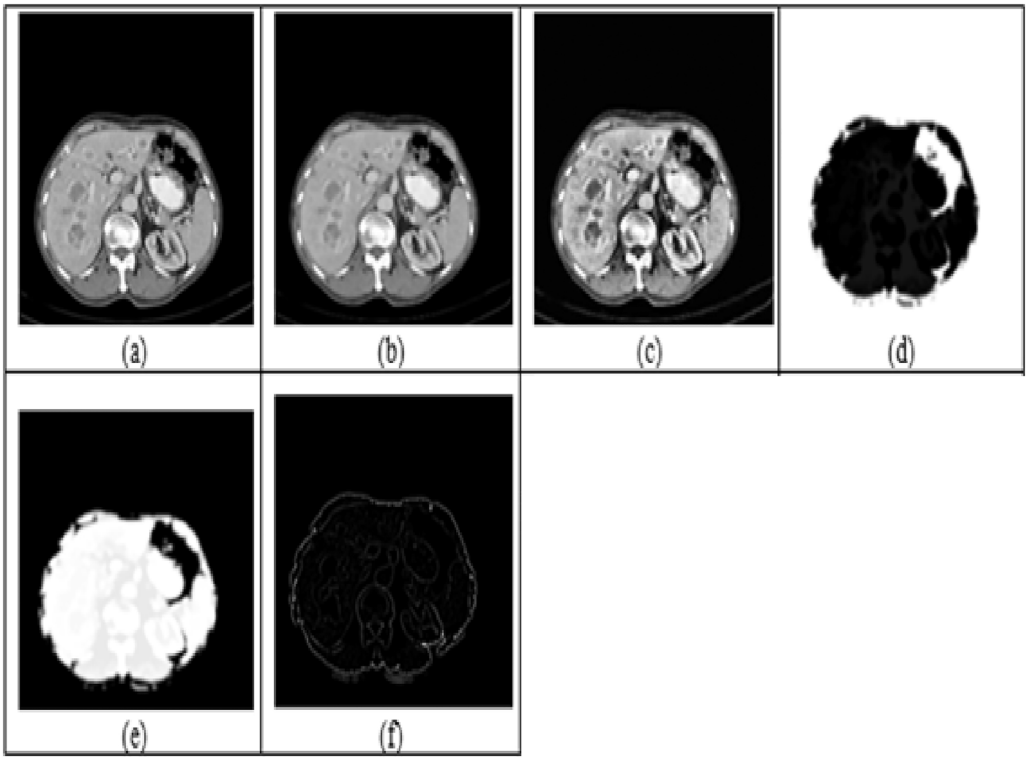

Fig. 3. The results of neutrosophic sets for liver CT image segmentation. (a) Original image, (b) image after applying median filter, (c) image after apply histogram equalization, (d) false Subset, (e) truth Subset, and (f) indeterminate Subset.

where $g(\bar{i}, j)$ is the local mean value of the pixels of the window size, and $Ho(i, j)$ is the homogeneity value of T at (i, j), which is described by the absolute value of difference between intensity $g(i, j)$ and its local mean value $g(\bar{i}, j)$. $\bar{g}_{\min}$ and $\bar{g}_{\max}$ are the first and last peaks respectively, calculated from the peaks greater than the mean of local maxima of image histogram. While $\bar{\text{Ho}}_{\min}$ and $\bar{\text{Ho}}_{\max}$ are the first and last peaks respectively, calculated from the homogeneity image using peaks greater than the mean of local maxima.

After the image is transformed to *NS* domain, some concepts and operations in the neutrosophic domain are defined and employed. Entropy is utilized to evaluate the distribution of different gray level in abdominal CT images.

Definition 2 (*Neutrosophy image entropy*). Image entropy is defined by summation of the three subsets entropies *I*, *F*, and *T*. [33]. If entropy is maximum, the different intensities have equal probability and the intensities distribute uniformly. If the entropy is small, the intensities have different probabilities and their distributions are non-uniform.

$$\mathbf{En_T} = -\sum \mathbf{P_T(i) \ln P_T(i)} \tag{6}$$

$$\mathbf{En_F} = -\sum \mathbf{P_F(i) \ln P_F(i)} \tag{7}$$

$$\mathbf{En_I} = -\sum \mathbf{P_I(i) \ln P_I(i)} \tag{8}$$

$$\mathbf{En_{NS}} = \mathbf{En_T} + \mathbf{En_I} + \mathbf{En_F} \tag{9}$$

where $\mathbf{En_I}$, $\mathbf{En_T}$ and $\mathbf{En_F}$ are the entropy of subsets *T*, *I* and *F*, respectively. $\mathbf{P_T(i)}$, $\mathbf{P_F(i)}$, and $\mathbf{P_I(i)}$ are the probabilities of element *i* in *T*, *I* and *F*. $\mathbf{En_I}$ is employed to evaluate distribution of indeterminacy, and $\mathbf{En_T}$ and $\mathbf{En_F}$ are utilized to measure the distribution of the elements in NS.

3.2. Watershed algorithm

Separating liver parenchyma from abdominal CT image is one of the more difficult processing operations. The watershed algorithm is often applied to this problem. Watershed image segmentation can be regarded as an image in three dimensions (two spatial coordinates versus intensity) [1]. We will use three types of the points which are *minimum*, *catchment basin*, and *watershed line* to express a topographic interpretation. Watershed algorithm has an advantage that it is fast speed, while a disadvantage of this algorithm is over-segmentation results. To solve this problem used marker-controlled for watershed segmentation. The watershed marker finds “catchment basins” and “watershed ridge lines”. The segmentation using watershed marker works better if you can identify, or “mark,” foregrounds objects and background locations.

3.3. Fast fuzzy c-mean algorithm (FFCM)

Fuzzy c-mean (FCM) is an unsupervised learning and a very common technique for statistical data analysis used in many fields, due to its overall performance. FCM is a generalization of the hard clustering scheme, also known as soft clustering, data elements can belong to more than one cluster which is determined by the degree of membership of the element in the corresponding cluster. FCM adopts fuzzy partitions of given data between 0 and 1 to determine the degree of its belonging to a group. To segment *N*-dimensional CT liver grayscaling image into c classes using a memory efficient implementation of the fuzzy c-means clustering algorithm named fast fuzzy c-means (FFCM). The computational efficiency is achieved by using the histogram of the image intensities during the clustering process instead of the raw image data. For more details in [34,35].

4. Proposed segmentation approach

Hybrid segmentation approach based on watershed algorithm, neutrosophic sets, and fast fuzzy c-means is proposed. The reason to do these integrations was that each technique as such has problems, which the other does not have. In general, the automatic hybrid CT liver segmentation approach introduced in this paper is composed of five phases as shown in Fig. 1 and the proposed approach steps are

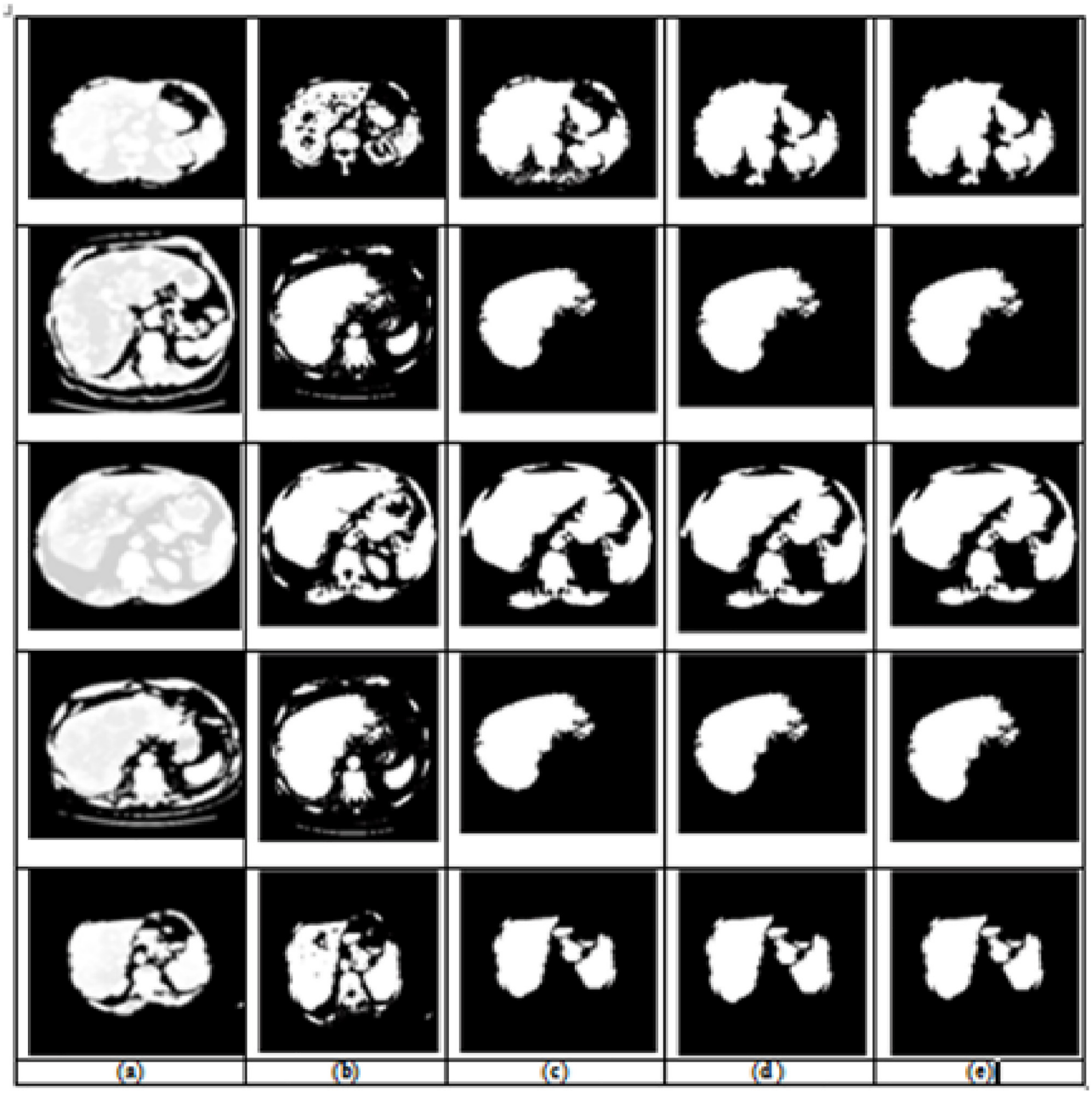

Fig. 4. Pre-segmentation results for liver from different CT images. (a) Truth image, (b) image after apply adaptive threshold, (c) image after fill holes and small objects are removed, (d) image after apply open and reconstruct, and (e) image after apply close and reconstruct.

illustrated in Algorithm 1.

Algorithm 1. NS and watershed model.

1: Convert image to gray scale and resize it to 64 × 64.
2: Apply median filter with 3 × 3 window to remove noise.
3: Apply histogram equalization to enhance contrast.
4: Convert each pixel of image to *NS*.
5: Calculate local maximum of histogram $g(\bar{i}, j)$ and find first peak $\bar{\text{Ho}}_{\min}$ and last peak $\bar{\text{Ho}}_{\max}$ greater than local mean.
6: $T(i, j)$ calculated from local of mean window, g_{min}, and g_{max}.
7: $I(i, j)$ calculated from homogeneity of subset T and difference between $g(i, j)$ and local mean value.
8: Calculate $F(i, j) = 1 - T(i, j)$.
9: Apply entropy En_{NS} to evaluate the indeterminacy in T, I, and F.
10: $En_{NS} = En_T + En_I + En_F$.
11: Apply adaptive threshold on *NS* image based on local mean intensity value.
12: Apply morphological operators open, erosion, close, dilation and fill holes.
13: Apply watershed algorithm using indeterminate and false subset images to control watershed.
14: Extract largest connected component from segmented image.
15: Apply FFCM on segmented liver to detect and segment tumors.
16: Apply morphological operators to remove non-tumor regions.

1. *Pre-processing*. In this phase, CT image firstly converted to gray-scale level and resized to reduce computation time. The median filter is applied to remove noise from CT image and contrast enhanced using histogram equalization.
   Fig. 2 shows the pre-processing stage on different CT slices. The gray-scale image is enhanced, smoothed and the noise is removed using median filter approach with window size 3 × 3. The filter runs through each element of the image and replace each pixel with the median of its neighboring pixels located in a square neighborhood around the evaluated pixel. Histogram equalization is used as seen in Eq. (10) to modify the dynamic range of the intensity values and

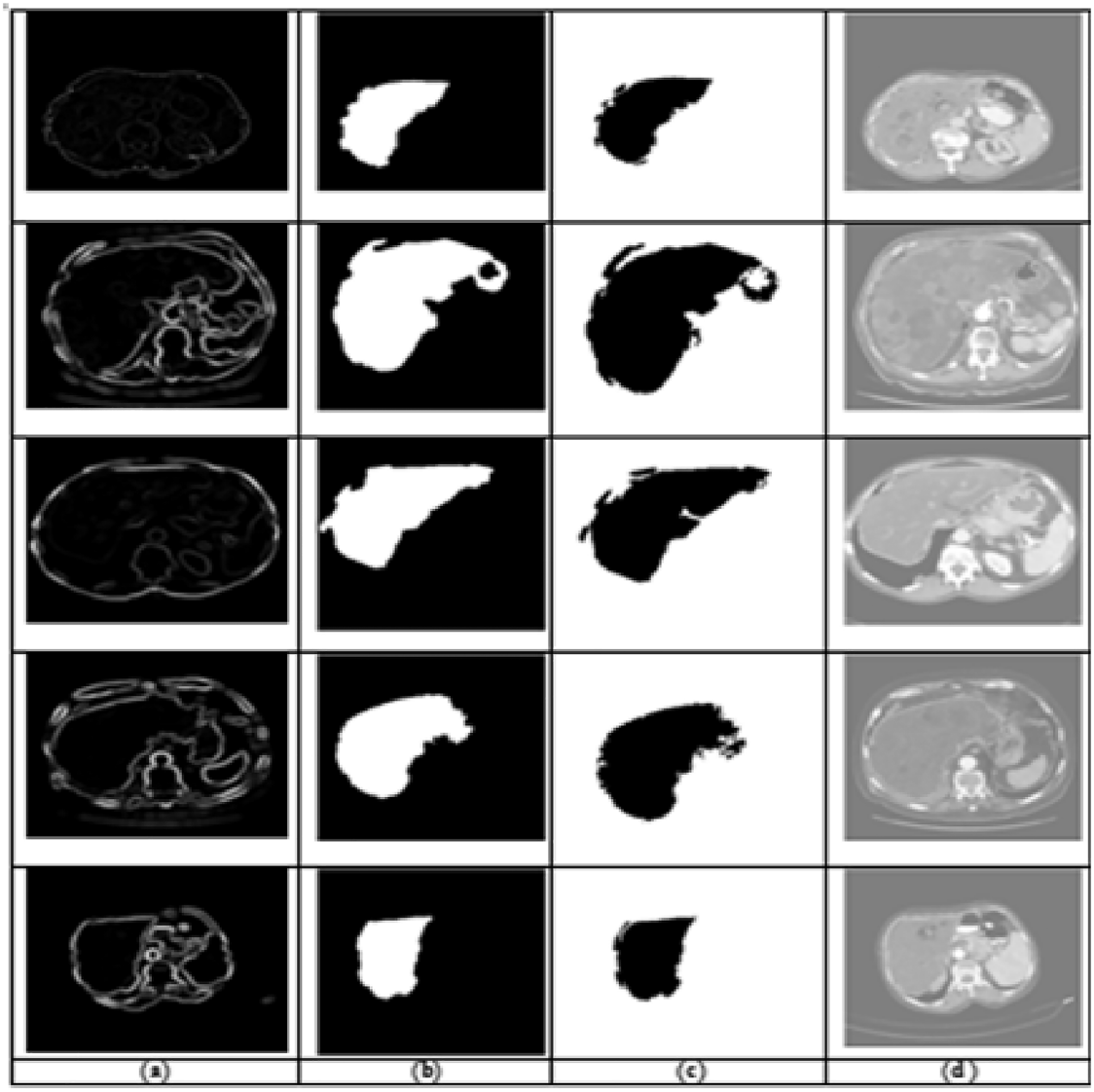

Fig. 5. Results of liver segmentation using watershed. (a) Indeterminate image, (b) foreground image, (c) background image, and (d) image after apply watershed.

increase the CT contrast without affecting the structure of the information contained therein.

$$H(v) = \text{round}\left(\frac{\bar{\text{cdf}}(v) - \bar{\text{cdf}}_{\min}}{(m \times n) - \bar{\text{cdf}}_{\min}} \times (L-2)\right) \tag{10}$$

cdf cumulative distribution function for unique pixel value v and L is the number of grey levels used of image of size $m \times n$.

2. *CT image transformation to NS domain*. Each pixel in the CT image will be converted to *NS* domain. That is mean each pixel will belong to either truth or false or indeterminate subsets in *NS* domain. Where indeterminate subset *I* represent foreground of the image, Truth subset *T* represent objects and finally False subset *F* represent the background of the image. After *NS* applied the truth subset image becomes more uniform and homogeneous, and more suitable for the segmentation process.
   Fig. 3 shows the results of the proposed approach based on neutrosophic sets for liver CT image segmentation on different patient's slices. In Fig. 3(b) pre-processing median filter approach is used to clear noise. In Fig. 3(c) contrast is enhanced using histogram equalization. The enhanced image is transformed to a false domain object as seen in Fig. 3(d). Fig. 3(e) shows the true domain objects. Fig. 3(f) shows the indeterminate domain objects. From the obtained results, the proposed NS approach is less sensitive to noise, gives clear noise and well-connected boundaries.
3. *Post-processing*. After liver CT images are converted to the neutrosophic domain, adaptive threshold based on local mean intensity value of the true image is used. Then, some morphological operators like open, erosion, close, dilation and fill holes are used to remove small objects and focus on liver parenchyma.
   After CT image is converted to the neutrosophic domain, adaptive threshold based on local mean intensity value of truth *NS* image is used. Fig. 4 shows the morphological operations open, close, reconstruct with shape and size of the structuring element (SE) that used to shrink and to remove small objects and extract liver from abdominal CT. The experimental results show that the best shape is diamond with SE size value 4.
4. *Liver parenchyma segmentation*. In this phase, the watershed algorithm is used to segment images. First control and mark foreground and background from *NS* image using subsets *I* for foreground objects and *F* for the background objects. Then watershed algorithm is applied to segment true images. After that the maximum region of interest (ROI) was selected to extract liver from abdominal CT using connected component algorithm.
   Fig. 5 shows the results of the watershed algorithm. It works on three images truth image after enhancement from previous steps,

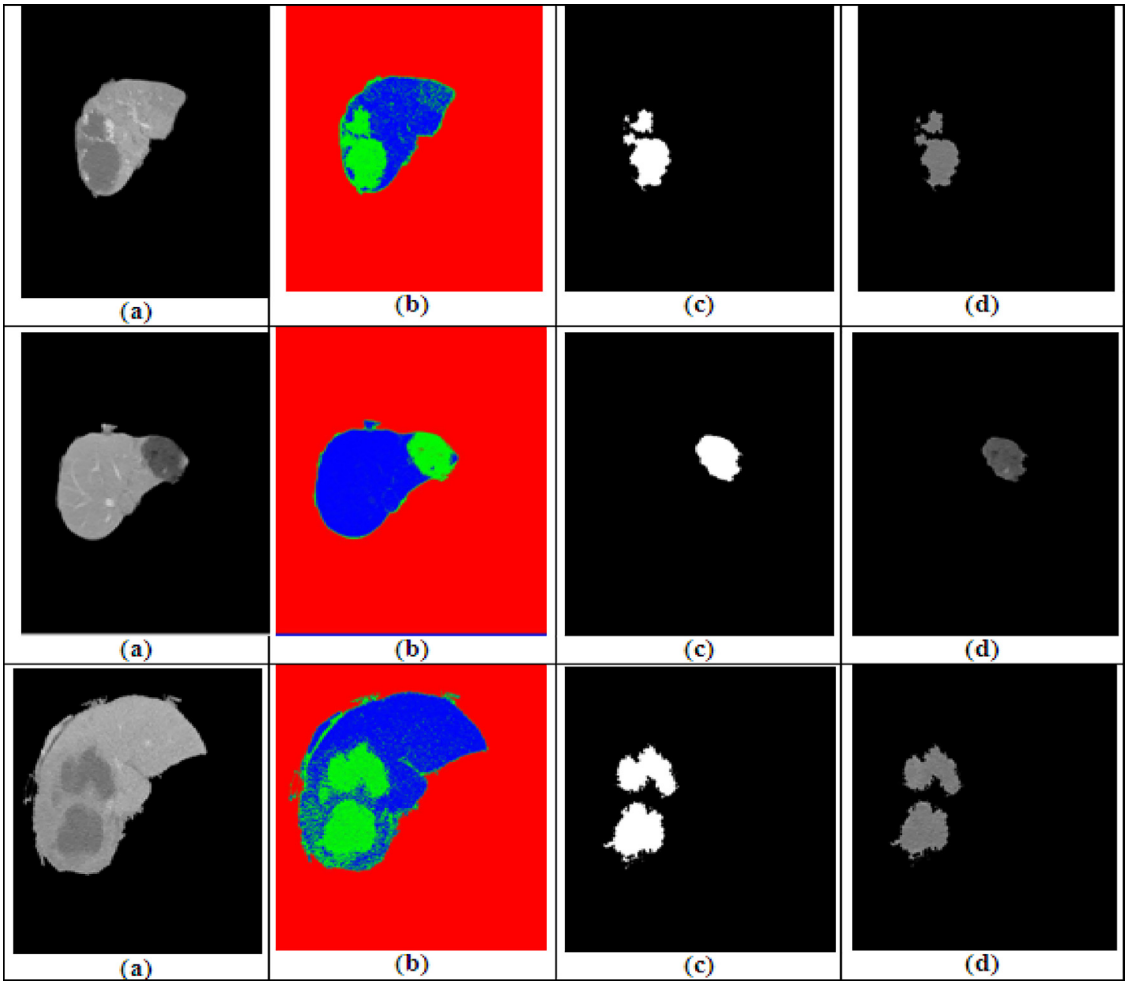

Fig. 6. Results of tumor segmentation using fast fuzzy c-means algorithm. (a) Segmented liver, (b) fast fuzzy c-means, (c) tumors segmentation using morphological operators, and (d) segmented tumors overlapped on original image.

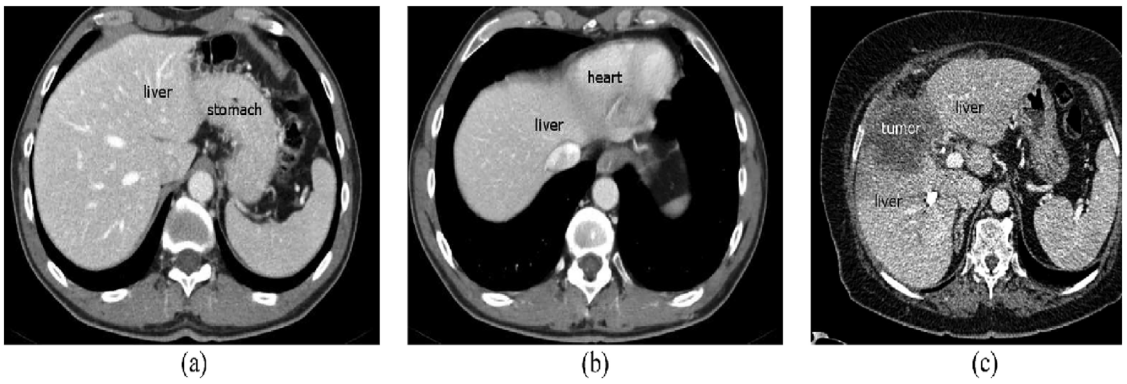

Fig. 7. Abdonial liver CT axial section, shows the liver nearby, same intensity and connected to other organs.

indeterminate subset, and False subset images. The Indeterminate and false images used as control marker for watershed. After that the maximum region of interest (ROI) selected and extracted from abdominal CT using connected component algorithm (CCL).

5. *Tumors segmentation and extraction*. In this phase, fast fuzzy c-means algorithm is applied on segmented liver parenchyma to detect and segment tumors from liver. Morphological operators are used to remover small objects which not represent tumors from liver.

Fig. 6 shows the segmentation of liver tumors (benign and malignant) using memory efficient implementation of the FCM called fast fuzzy c-means algorithm (FFCM). The proposed FFCM provides excellent results for tumor clustering and segmentation without any loss of tumor detection with high accuracy. Also false positive regions that affect system performance are reduced.

5. Experimental results and discussion

5.1. Description of CT liver data set and computer setting

The proposed approach will be applied on a complex dataset. The

Table 2
The results of the proposed approach, adaptive threshold, and region growing for liver CT image segmentation using Jaccard Index, correlation, and dice coefficient.

Im.	NS-WS-FFCM			Adaptive threshold			Region growing		
	Jaccard	Dice	Corr	Jaccard	Dice	Corr	Jaccard	Dice	Corr
1	0.7794	0.876	0.863	0.7589	0.863	0.729	0.6499	0.788	0.92
2	0.904	0.95	0.945	0.675	0.806	1.038	0.779	0.876	0.92
3	0.9117	0.954	0.944	0.9283	0.963	0.686	0.7867	0.881	0.946
4	0.8281	0.906	0.895	0.7627	0.865	0.739	0.7031	0.826	0.642
5	0.8969	0.946	0.933	0.7219	0.838	0.888	0.7719	0.871	0.923
6	0.8921	0.943	0.935	0.7273	0.842	0.898	0.7671	0.868	0.79
7	0.8072	0.893	0.886	0.7734	0.872	0.767	0.6797	0.809	0.766
8	0.9335	0.966	0.963	0.8164	0.899	0.828	0.7985	0.888	0.803
9	0.9055	0.95	0.947	0.7988	0.888	0.886	0.7805	0.877	0.906
10	0.8895	0.942	0.928	0.9419	0.97	0.76	0.7645	0.867	0.768
11	0.92	0.958	0.951	0.8666	0.929	0.647	0.795	0.886	0.691
12	0.7482	0.856	0.846	0.7779	0.875	0.768	0.6207	0.766	0.605
13	0.8802	0.936	0.924	0.7261	0.841	0.888	0.7552	0.861	0.807
14	0.9333	0.965	0.962	0.6994	0.823	1.071	0.7983	0.888	0.783
15	0.7778	0.875	0.862	0.7666	0.868	0.783	0.6628	0.797	0.938
16	0.8675	0.929	0.912	0.8034	0.891	0.832	0.7455	0.854	0.814
17	0.8522	0.92	0.914	0.7719	0.871	0.768	0.7312	0.845	0.912
18	0.9097	0.953	0.941	0.7693	0.87	0.74	0.7747	0.873	0.809
19	0.9166	0.957	0.943	0.6933	0.819	1.001	0.7876	0.881	0.794
20	0.8354	0.91	0.898	0.675	0.806	1.026	0.7104	0.831	0.944
21	0.8459	0.916	0.908	0.7962	0.887	0.786	0.7288	0.843	0.943
22	0.8597	0.925	0.906	0.7279	0.843	0.895	0.7337	0.846	0.909
23	0.7988	0.888	0.846	0.9036	0.949	0.694	0.6878	0.815	0.781
24	0.879	0.936	0.919	0.8106	0.895	0.83	0.754	0.86	0.622
25	0.9319	0.965	0.954	0.7059	0.828	1.072	0.7909	0.883	0.915
26	0.8428	0.915	0.885	0.7691	0.869	0.759	0.7278	0.842	0.943
27	0.8871	0.94	0.935	0.7789	0.876	0.764	0.7741	0.873	0.805
28	0.8841	0.938	0.93	0.6767	0.807	1 063	0.7601	0.864	0.817
29	0.8933	0.944	0.932	0.7841	0.879	0.78	0.7653	0.867	0.944
30	0.8414	0.914	0.891	0.6794	0.809	1.075	0.7224	0.839	0.821

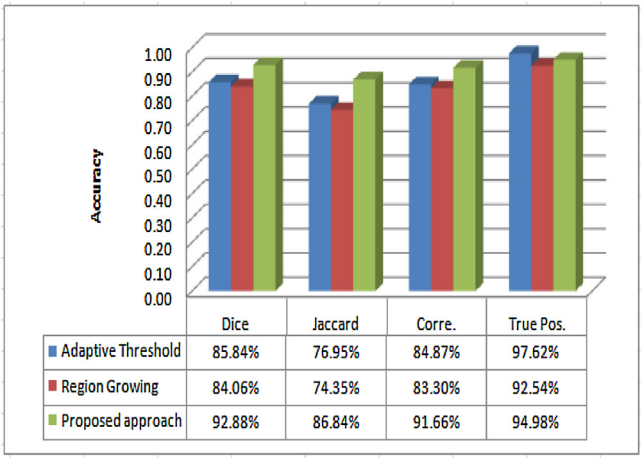

Fig. 8. Visual representation and comparison between the accuracy obtained from the proposed approach, adaptive threshold and region growing in terms of correlation, true positive, dice coefficient, and Jaccard Index.

dataset contains more than 105 patients have CT for liver abdominal and more than one hundred fifty slices for each patients. All images are in JPEG format, extracted from a DICOM file with dimensions 630 × 630 and bit depth 24 bits [1]. In abdominal liver CT images, liver is connected to other tissues such as spleen, stomach, kidney, gallbladder, gastrointestinal tract, and spinal muscles. The intensity distribution is different between slices and the variation in intensities may cause the segmentation very hard and leak. Fig. 7 shows the overlap in abdominal CT axial section between the intensity of liver and other nearby tissues with strong connections with liver. The proposed approach is tested on difficult data set and the accuracy results compared with adaptive threshold, and Region growing algorithms. All algorithms are tested on the same data set. In all cases, the image segmentation approaches were programmed in MATLABR 2007 on a computer having Intel Core I7 and 8 GB of memory.

5.2. Performance measures

In order to verify the quality of CT image segmentation using the proposed approach and to compare it with other algorithms. A quantitative analysis is carried out using six indices: Jaccard Index [35], dice coefficient [35], entropy-based metric (E_n) [36], partition coefficient (V_{pc}) [37], and partition entropy (V_{pe}) [37]. These indices are calculated as follow:

Jaccard index is very popular and used as a similarity index for binary data **asshowninthefollowingform**.

$$J(\mathrm{OA}) = \frac{A \cap B}{A \cup B} \tag{11}$$

OA is the area of overlap; *A* is binary image and *B* is ground truth image.

Dice coefficient is defined as follows:

$$D(A, B) = \frac{2|A \cap B|}{|A| + |B|} \tag{12}$$

The dice coefficient is commonly used to measure the performance of segmentation. Its values range between 0 and 1 which means 0 is no overlap and 1 is perfect agreement.

Correlation coefficient (CC) used to measure the similarity between the segmented imaged and ground truth in relation with their respective pixel intensity. *CC* is defined as follow.

$$\mathrm{CC} = \frac{\sum_i \sum_j (A_{\mathrm{ij}} - \mathrm{mean}(A))(B_{\mathrm{ij}} - \mathrm{mean}(B))}{\sqrt{\left(\sum_i \sum_j (A_{\mathrm{ij}} - \mathrm{mean}(A))^2\right)\left(\sum_i \sum_j (B_{\mathrm{ij}} - \mathrm{mean}(B))^2\right)}} \tag{13}$$

where the subscript indices *m* and *n* refer to the pixel location in the image.

Partition coefficient (V_{pc}) and *partition entropy* (V_{pe}) are two indices used to validate the fuzzy c-means clustering algorithm based on the elements of the membership matrix.

$$V_{\mathrm{pc}} = \frac{1}{n} \sum_{i=1}^{c} \sum_{j=1}^{n} \mu_{\mathrm{ij}}^2 \tag{14}$$

where $\frac{1}{c} \le V_{\mathrm{pc}} \le 1$. The PC index indicates the average contents of pairs of fuzzy subsets in fuzzy partition by combining into a single number.

$$V_{\mathrm{pe}} = -\frac{1}{n} \sum_{i=1}^{c} \sum_{j=1}^{n} \mu_{\mathrm{ij}} \log \mu_{\mathrm{ij}} \tag{15}$$

V_{pe} measures the fuzziness of the cluster partition similar to the partition coefficient. An optimal clusters obtained by minimizing to produce the best clustering performance for the data.

Entropy-based metric (E_n). Entropy used for measuring the uniformity of pixel characteristics within a segmentation region and for measuring the complexity of the division of the image into regions based on information theory. The entropy of every region *j* is defined as follows.

$$H(R_j) = -\sum_{m \in V_j} \frac{L_j(m)}{S_j} * \log \frac{L_j(m)}{S_j} \tag{16}$$

where V_j is the set of all possible in region *j*, $L_j(m)$ is the number of pixels belonging to region *j* with feature *m*, and S_j is the area of region *j*.

The expected region entropy of the CT image *I* and the expected entropy of the other regions is used to measure the uniformity within the regions of *I* as follows:

$$H_r(I) = \sum_{j=1}^{c} \left(\frac{S_j}{S_I}\right) * H(R_j) \tag{17}$$

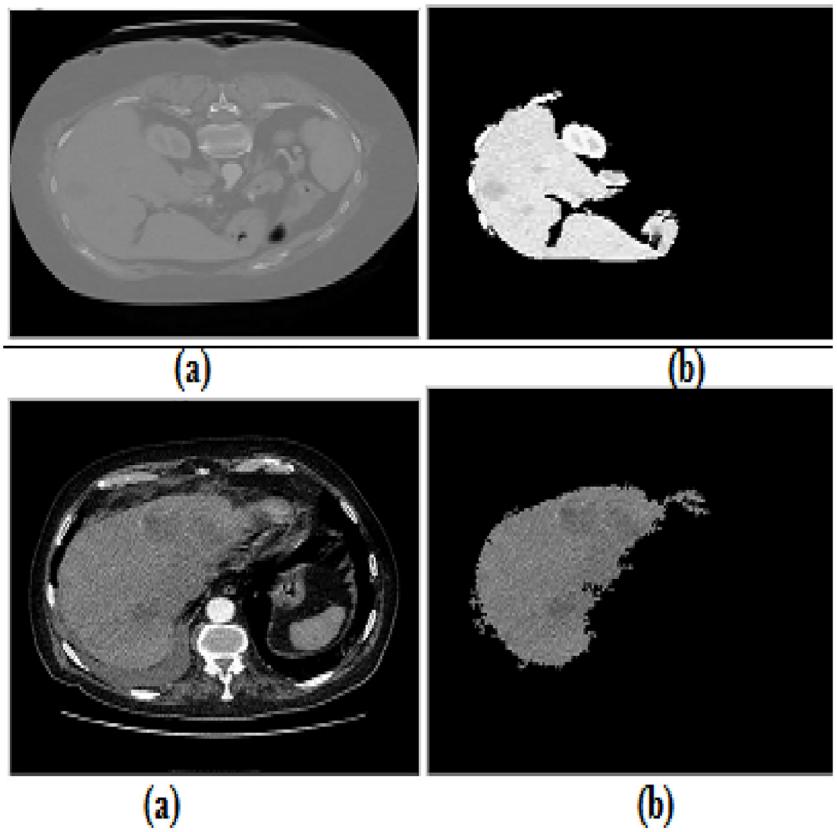

Fig. 9. Results of different abdominal CT images to prove the proposed approach is less sensitive to noise to extract liver parenchyma. (a) Original noisy image and (b) liver segmentation.

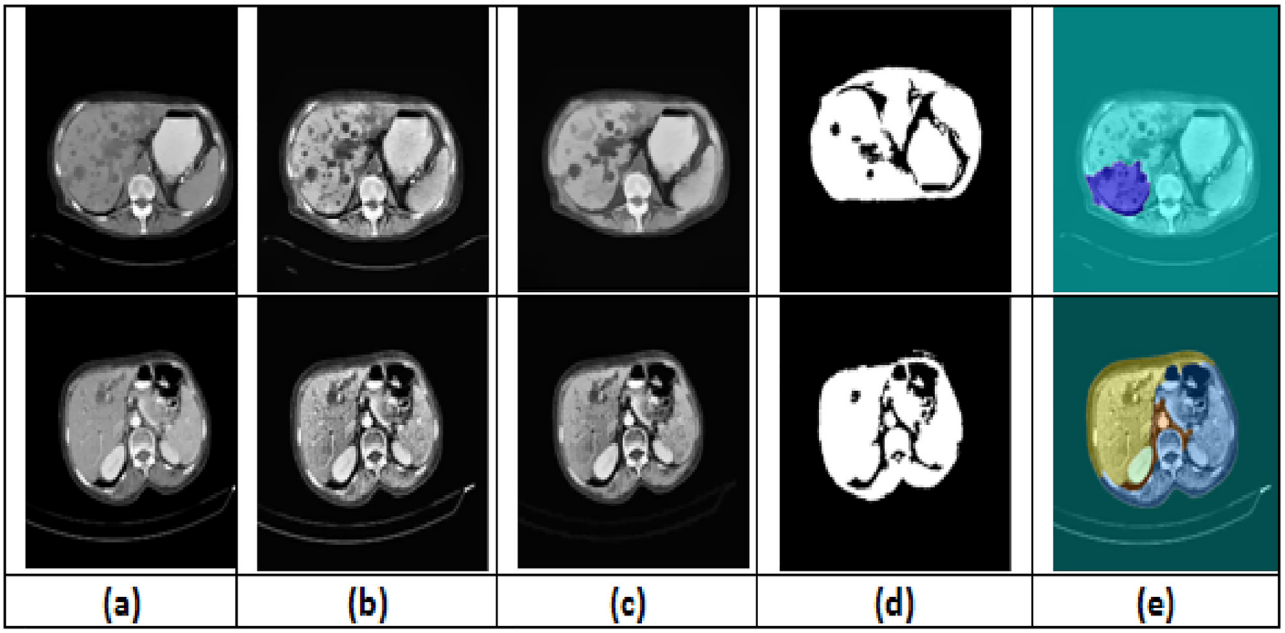

Fig. 10. The results of using watershed only. (a) Original CT image, (b) histogram equalization, (c) morphological operators, (d) adaptive thresholding, (e) watershed segmentation.

The entropy layout entropy is used to counteract the effects of over-segmenting and under-segmenting. layout entropy can be calculated as follow:

$$H_L(I) = -\sum_{j=1}^{c}\left(\frac{S_I}{S_I}\right)^{*}\log\frac{S_I}{S_I} \tag{18}$$

From these two factors entropy-based evaluation function is calculated E. The measure E yields smaller value for better segmentation and higher otherwise calculated as follow:

$$E = H_r(I) + H_L(I) \tag{19}$$

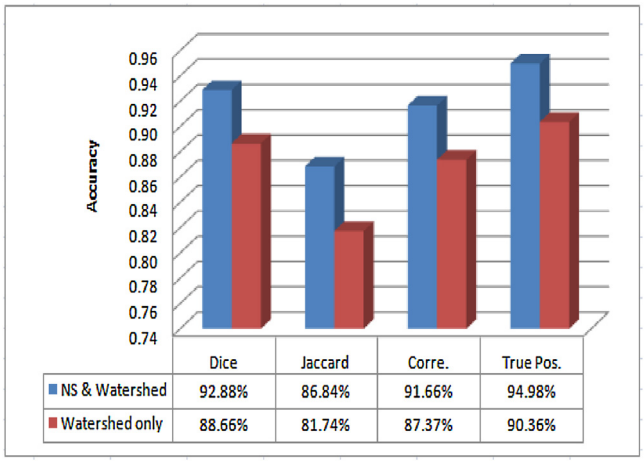

	Dice	Jaccard	Corre.	True Pos.
NS & Watershed	92.88%	86.84%	91.66%	94.98%
Watershed only	88.66%	81.74%	87.37%	90.36%

Fig. 11. Visual representation and Comparison between the proposed neutrosophic set and watershed approach with watershed algorithm only.

5.3. Results and discussion

The proposed approach uses a novel concept of neutrosophic sets and adaptive watershed segmentation algorithm for automatic extract liver tumors from abdominal CT images. It obtains overall accuracy almost 95%. This result is better compared to adaptive threshold and region growing algorithm.

Table 2 shows the comparison between the proposed approach, adaptive threshold [32] and region growing [38] for liver segmentation. In addition Fig. 8 shows the visual representation for the best similarity indices's in terms of Dice Coefficient, Jaccard Index, and Correlation. As can be seen, the proposed approach acts pretty and better accuracy for all measurements followed by adaptive threshold which select an individual threshold for each pixel based on the range of intensity values in its local neighborhood, this is make intensity histogram does not contain distinctive peaks. Also it is more sophisticated and accommodate changing lighting conditions in the image. The main drawback of this method is that, it is computational expensive and not appropriate for real-time applications.

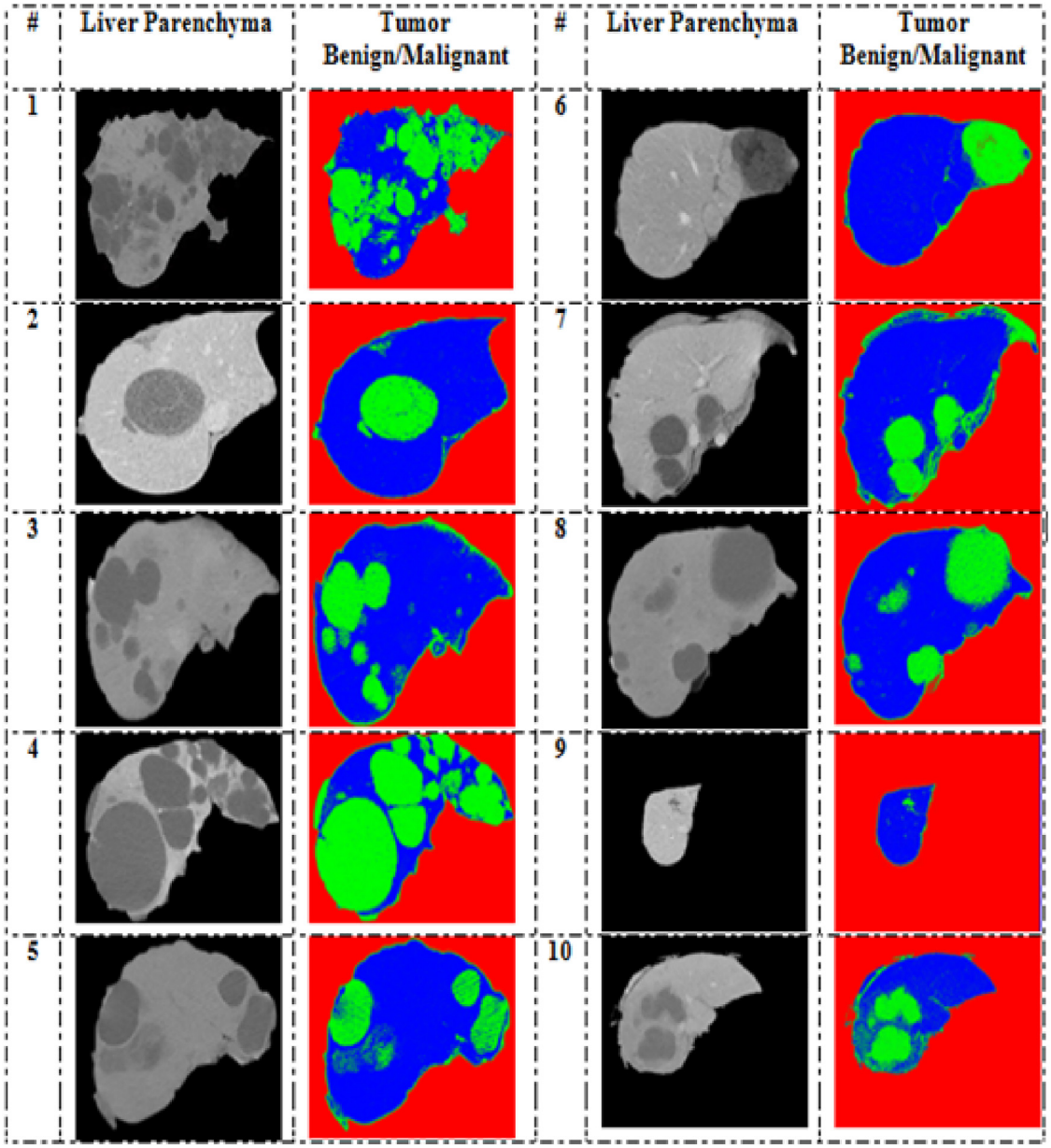

Fig. 12. Sample results of the proposed approach for different patient's liver tumors.

Table 3
Internal validity cluster indices evaluation using partition coefficient (V_{pc}), partition entropy (V_{pe}), and entropy-based metric (E_n).

Im.	V_{pc}	V_{pe}	E_n
1	0.416932	0.341636	1.07269
2	0.421026	0.32572	0.859855
3	0.413901	0.359581	1.601528
4	0.413554	0.352702	1.09138
5	0.357888	0.397455	1.046865
6	0.465071	0.326871	1.006505
7	0.349194	0.35701	1.236447
8	0.456346	0.278621	0.672169
9	0.441919	0.337476	0.98584
10	0.39423	0.371347	1.646975
11	0.412318	0.358495	1.289047
12	0.432716	0.298588	-1.192729
13	0.370576	0.385847	1.081468
14	0.458046	0.303049	0.746747
15	0.485352	0.356641	1.20805
16	0.468327	0.282769	0.734358
17	0.467896	0.282687	−1.26104
18	0.469732	0.277711	−1.18394
19	0.449559	0.34278	0.817948
20	0.463941	0.292219	0.830245
21	0.475224	0.287913	0.736041
22	0.459588	0.330357	1.014164
23	0.430036	0.352068	1.448281
24	0.468102	0.277782	0.699572
25	0.446393	0.312698	0.793044
26	0.356865	0.362553	1.175963
27	0.384426	0.3180.15	1.288198
28	0.4026	0.327779	0.955975
29	0.472108	0.278973	1.209227
30	0.388055	0.343446	0.790185

Absence of clear edges, definite shape of liver parenchyma and close connection between liver tissue and other organs will limit the liver parenchyma to segment and extract based on edge algorithm. Fig. 9, proves our proposed approach for the noisy liver CT images. The results prove that, the proposed NS approach is not sensitive to noise and extract liver parenchyma from abdominal CT images without loss of information.

Fig. 10 shows the results of using Watershed algorithm only to segment liver from abdominal CT. Fig. 11 shows the comparison between proposed neutrosophic sets and watershed approach with only watershed algorithm in terms of dice coefficient, Jaccard Index, correlation and true positive.

The best results for liver tumor detection and segmentation for different patients using the proposed approach can be seen in Fig. 12. The segmentation results show that, high accuracy obtained without any loss of information. Table 3 shows the validity clusters indices for the centroids selected automatically using the proposed approach. We can see from the partition coefficient index (V_{pc}) that the best clusters are selected from with high maximum values of V_{pc} which indicate to the best and compact clusters. In the partition entropy validity Index (V_{pe}) the best and maximum values obtained from the proposed approach which indicates to the optimal clusters centroid obtained. The entropy based metric validity index (E_n) yields smaller value for effectiveness and better segmentation. From Table 3, we can see that the best segmentation with smaller En is obtained from the proposed approach. From the analysis and quantitative evaluation we can see that the proposed approach is superior with good segmentation results and can help doctor to detect liver tumor.

Table 4 shows the comparison between the proposed segmentation approach with other previous work on liver CT images. Moreover, characteristics of the works, datasets, and algorithms that are used for segmentation, and accuracy of segmentation are shown. As can be seen, the proposed approach acts pretty and better than other works on the same and different datasets with overall accuracy almost 95%. The same accuracy obtained from the proposed approach by Siri et al. [42] using the neutrosophic sets and Chan-Vese, followed by the approach proposed by Mostafa et al. in [46] using bio-inspired ant lion optimization algorithm and morphological operator, followed by the approach proposed by Anter et al. in [5] and Sayed et al. in [33]. From the comparisons, we can demonstrate that the neutrosophy can reduce over-segmentation, effective, robust, and it can handle uncertainty and indeterminacy in CT images.

6. Conclusion and future work

We proposed a hybrid segmentation approach using neutrosophic sets, watershed algorithm, and fast fuzzy c-means algorithm for automatic liver tumor segmentation from abdominal CT images. The experiments demonstrate that the proposed approach based on neutrosophy can handle indeterminacy and uncertainty better, reduce over-segmentation and has good accuracy and performance on non-uniform and noisy images. The overall accuracy obtained from the proposed approach almost 95% of good liver segmentation. This result can help for further diagnosis and treatment planning. In the future work, we plan to apply the proposed neutrosophy segmentation approach on a huge number of CT images to evaluate the performance.

Table 4
Comparison between proposed approach with other existing work on liver segmentation.

Authors	Year	Data set		Acc.	Methodology
		No.	Description		
Jeongjin et al. [16]	2007	20	Private	70%	region growing, level-set
Ruchaneewan et al. [17]	2007	30	MICCAI	86%	Intensity-based partition, region based texture, and thresholding
Abdalla et al. [31]	2012	26	Hospital data (Private)	84%	Region growing, CCL, and morphological operators
Abdalla et al. [39]	2012	27	Hospital data(Private)	92%	Level set and watershed
Anter et al. [1]	2013	112	Radiopaedia &ISIS center	93%	watershed algorithm, RG, and CCL
Aldeek et al. [40]	2014	44	–	87%	Markov random field, gradient vector flow (GVF), and Bayesian classifier
Siri et al. [41]	2017	108	M/S CT scan Centre	91.61%	NS and fast marching method
Siri et al. [42]	2017	110	M/S CT scan Centre	95%	NS and Chan-Vese
Anter et al. [1]	2013	112	Radiopaedia &ISIS center	93%	watershed algorithm, RG, and CCL
Anter et al. [5]	2014	30	Radiopaedia	94%	NS and FCM
Sayed et al. [43]	2016	30	Radiopaedia	94%	FCM and GWO
Sayed et al. [44]	2016b	30	Radiopaedia	90.89%	PSO
Ali et al. [45]	2016	30	Radiopaedia	92.66%	FCM and GWO
Mostafa et al. [46]	2018	30	Radiopaedia	94.49%	ALO and morphological operators
Mostafa et al. [47]	2016	38	Radiopaedia	93.73%	RG, ABC, and morphological operators
Proposed approach	2017	30	Radiopaedia	95%	NS, watershed, adaptive threshold, FFCM

References

[1] Anter A, Azar A, Hassanien A, El-Bendary N, ElSoud M. Automatic computer aided segmentation for liver and hepatic lesions using hybrid segmentations techniques. IEEE proceedings of federated conference on computer science and information systems 2013:193–8.
[2] Priyadarsini S, Selvathi D. Survey on segmentation of liver from CT images. 2012 IEEE international conference on advanced communication control and computing technologies (ICACCCT). 2012. p. 234–8.
[3] Hassan, Elmogy, Sallam. Medical image segmentation for liver diseases: a survey. Int J Comput Appl 2015;118(19).
[4] Cheng D, Guot Y, Zhang Y. A novel image segmentation approach based on neutrosophic set and improved fuzzy c-means algorithm. N Math Nat Comput 2011;7(1):155–71.
[5] Anter A, Hassenian A, AbuElSoud M. Neutrosophic sets and fuzzy c-means clustering for improving CT liver image segmentation. 5th Int Conf innovations in bio-inspired computing and applications, IBICA2014, vol. 303. 2014. p. 193–203.
[6] Moltz JH, Bornemann L, Dicken V, Peitgen H. Segmentation of liver metastases in CT scans by adaptive thresholding and morphological processing. MICCAI workshop, vol. 41, no. 43 2008:195.
[7] Wong D, Liu J, Fengshou Y, Tian Q, Xiong W, Zhou J, Wang SC. A semi-automated method for liver tumor segmentation based on 2D region growing with knowledge-based constraints. MICCAI workshop, vol. 41, no. 43 2008:159.
[8] Li Bing Nan, Chui Chee Kong, Ong SH, Chang Stephen. Integrating FCM and level sets for liver tumor segmentation. 13th international conference on biomedical engineering. 2009. p. 202–5.
[9] Smeets D, Loeckx D, Stijnen B, De Dobbelaer B, Vandermeulen D, Suetens P. Semi-automatic level set segmentation of liver tumors combining a spiral-scanning technique with supervised fuzzy pixel classification. Med Image Anal 2010;14(1):13–20.
[10] Moghe AA, Singhai J, Shrivastava SC. Automatic threshold based liver lesion segmentation in abdominal 2D-CT images. Int J Image Process 2011;5(2):166.
[11] Nural W, Hans B. Integration of Morphology and Graph-based Techniques for Fully Automatic Liver Segmentation. Majlesi J Electr Eng 2010;4(3):59–66.
[12] Kumar SS, Moni RS, Rajeesh J. Automatic Liver and Lesion Segmentation: A Primary Step in Diagnosis of Liver Diseases vol. 7. SIViP, Springer; 2013. p. 163–72.
[13] Badura P, Pietka E. 3D fuzzy liver tumor segmentation. Inform Technol Biomed 2012;7339:47–57.
[14] Lim SJ, Jeong YY, Ho YS. Segmentation of the liver using the deformable contour method on CT images. PCM, Springer; 2005. p. 570–81.
[15] Huang C, Jia F, Li Y, Zhang X, Luo H, Fang C, Fan Y. Automatic liver segmentation based on shape constrained differeomorphic demons atlas registration. Proceedings of the 2012 international conference on electronics, communications and control. 2012. p. 126–9.
[16] Jeongjin L, Namkug K, Ho L, Joon B, Hyung J, Yong M, Yeong S, Hong K. Efficient liver segmentation using a level-set method with optimal detection of the initial liver boundary from level-set speed images. Comput Methods Programs Biomed 2007;88:26–38.
[17] Ruchaneewan S, Daniela S, Jacob F. A hybrid approach for liver segmentation. 3D segmentation in the clinic: a grand challenge. Intelligent Multimedia Processing Laboratory; 2007. p. 151–60.
[18] Campadelli P, Casiraghi E, Pratissoli S, Lombardi G. Automatic abdominal organ segmentation from CT images. Electron Lett Comput Vis Image Anal 2009;8(1):1–14.
[19] Campadelli P, Casiraghi E, Esposito A. Liver segmentation from computed tomography scans: a survey and a new algorithm. Artif Intell Med 2009;45(2-3):185–96.
[20] Lu J, Wang D, Shi L, Heng PA. Automatic liver segmentation in CT images based on support vector machine. Proceedings of the IEEE-EMBS international conference on biomedical and health informatics 2012:333–6.
[21] Kaur R, Kaur L, Gupta S. Enhanced K-mean clustering algorithm for liver image segmentation to extract cyst region. IJCA special issue on novel aspects of digital imaging applications (DIA) (I) 2011:59–66.
[22] Zhao Y, Zan Y, Wang X, Li G. Fuzzy C-means clustering-based multilayer perceptron neural network for liver CT images automatic segmentation. Control and decision conference (CCDC). 2010. p. 3423–7. [Chinese].
[23] Hame Y. Liver tumor segmentation using implicit surface evolution. The Midas journal (2008 MICCAI workshop) 2008:1–10.
[24] Ciecholewski M, Ogiela MR. Automatic segmentation of single and multiple neoplastic hepatic lesions in CT images. International work-conference on the interplay between natural and artificial computation. 2007. p. 63–71.
[25] Taieb Y, Eliassaf O, Freiman M, Joskowicz L, Sosna J. An iterative Bayesian approach for liver analysis: tumors validation study. MICCAI workshop, vol. 41 2008:43.
[26] Zhang X, Tian J, Xiang D, Li X, Deng K. Interactive liver tumor segmentation from ct scans using support vector classification with watershed. 2011 annual international conference of the IEEE on Engineering in Medicine and Biology Society, EMBC. 2011. p. 6005–8.
[27] Patil S, Udupi V, Patole D. A Robust system for Segmentation of primary Liver Tumor in CT images. Int J Comput Appl 2013;75(13):6–10.
[28] Kumar S, Moni R. Diagnosis of liver tumor from ct images using curvelet transform. Int J Comput Sci Eng 2010;2(4):1173–8.
[29] Saxena S, Sharma N, Sharma S, Singh S, Verma A. An automated system for atlas based multiple organ segmentation of abdominal CT images. BJMCS 2016;12:1–14.
[30] Zhang M, Zhang L, Cheng D. A neutrosophic approach to image segmentation based on watershed method. Signal processing vol. 90. Elsevier; 2010. p. 1510–7.
[31] Abdalla M, Hesham H, Neven I, Hassenian A, Gerald S. Evaluating the effects of image filters in CT liver CAD system. Proceeding of IEEE-EMBS international conference on biomedical and health informatics. 2012.
[32] Anter M, Ahmed Hassenian A, ElSoud M, Azar A. Automatic liver parenchyma segmentation system from abdominal CT scans using hybrid techniques. Int J Biomed Eng J Technol 2014;17(2):148–67.
[33] Guo Y, Cheng D, Zhang Y, Zhao W. A new neutrosophic approach to image thresholding. N Math Nat Comput 2008;4(3):291–308.
[34] Ali AR, Couceiro M, Anter AM, Hassenian AE. Evaluating an evolutionary particle swarm optimization for fast fuzzy c-means clustering on liver CT images. Comput Vis Image Process Intell Syst Multimedia Technol 2014;Vo.1.
[35] Anter AM, Hassenian AE. Computational intelligence optimization approach based on particle swarm optimizer and neutrosophic set for abdominal CT liver tumor segmentation. J Comput Sci 2018;25:376–87.
[36] Elazab A, Wang C, Jia F, Wu J, Li G, Hu Q. Segmentation of brain tissues from magnetic resonance images using adaptively regularized kernel-based fuzzy-means clustering. Comput Math Methods Med 2015;Volume 2015:1–12. ID 485495.
[37] Prabu C, Bavithiraja SVMG, Narayanamoorthy S. A novel brain image segmentation using intuitionistic fuzzy C means algorithm. Int J Imag Syst Technol 2016;26(1):24–8.
[38] Alazab M, Mofakharul I, Sitalakshmi V. Towards automatic image segmentation using optimised region growing technique. Advances in artificial intelligence. Springer Berlin Heidelberg; 2009. p. 131–9.
[39] Abdalla Z, Neveen I, Hassenian A, Hesham A. Level set-based CT liver image segmentation with watershed and artificial neural networks. IEEE; 2012. p. 96–102.
[40] Aldeek N, Alomari R, Al-Zoubi M, Hiary H. Liver segmentation from abdomen CT images with Bayesian model. J Theor Appl Inform Technol 2014;60(3):483–90.
[41] Siri SK, Latte MV. A novel approach to extract exact liver image boundary from abdominal CT scan using neutrosophic set and fast marching method. J Intell Syst 2017:1–16.
[42] Siri SK, Latte MV. Combined endeavor of neutrosophic Set and Chan-Vese model to extract accurate liver image from CT scan. Comput Methods Programs Biomed 2017;151:101–9.
[43] Sayed GI, Hassanien AE, Schaefer G. An automated computer-aided diagnosis system for abdominal CT liver images. Procedia Comput Sci 2016;90:68–73.
[44] Sayed GI, Hassanien AE. Abdominal CT liver parenchyma segmentation based on particle swarm optimization. The 1st international conference on advanced intelligent system and informatics (AISI2015). 2016. p. 219–28.
[45] Ali AF, Mostafa A, Sayed GI, Elfattah MA, Hassanien AE. Nature inspired optimization algorithms for CT liver segmentation. Medical imaging in clinical applications 2016:431–60.
[46] Mostafa A, Houssein EH, Houseni M, Hassanien AE, Hefny H. Evaluating swarm optimization algorithms for segmentation of liver images. Advances in soft computing and machine learning in image processing 2018:41–62.
[47] Mostafa A, Fouad A, Elfattah MA, Hassanien AE, Hefny H. Artificial bee colony based segmentation for CT liver images. Medical imaging in clinical applications 2016:409–30.